A Supramolecule-Triggered Mechanochromic Switch of Cyclodextrin-Jacketed Rhodamine and Spiropyran Derivatives

*Shulin Wan, Zhiyong Ma, Chen Chen, Fangfei Li, Feng Wang, Xinru Jia, Wantai Yang, and Meizhen Yin**

An innovative approach for covalent-bond-activated mechanoresponse by complexing rhodamine or spiropyran with cyclodextrin (CD) is reported. This approach endows diverse fluorophores with perfect mechanochromism by introducing a supramolecular system. Unique characteristics such as noncovalent chemical modification and convenient preparation make this approach promising for practical applications. The strong hydrogen bonds provided by CD play a crucial role in triggering the mechanochromic switch. First, the hydrogen bonds seize both sides of the fluorophore's weak chemical bonds and tightly lock the fluorophore in the cavity of CD. Second, the hydrogen bonds prompt the aggregation of complex inclusions in large ordered arrays and strengthen the molecular interactions. In this way, the weak chemical bonds can focus more external force and stretch more easily upon shearing (quantified). This is the first report of supramolecule-triggered mechanochromic switches. This study opens an avenue to correlate a mechanochemical reaction with a supramolecular system.

1. Introduction

Mechanochromic luminescent materials have attracted much attention because of their essential roles in the memory devices, sensors, security materials, and informational display areas.[1] Normally, two predominant approaches are applied to obtain these materials. One is monitoring the microstructures of the molecular assemblies,[2] and the other is changing the chemical structures by mechanical stimuli, which induces color changes by breaking the chemical bonds.[3] In recent years, the latter approach is appealing to more researchers due to the good color stability and significant color transformation.[3d] Reported achievements of the activation of mechanoresponsive molecules by covalent bonds can be summarized into two classifications. The first is covalently modifying the molecules, especially with numerous hetero atoms, to facilitate the interactions such as hydrogen bonds, π–π stacking, and van der Waals force between molecules. These covalent chemical modifications require complicated syntheses. Moreover, although some molecules are elaborately modified, a high (nonquantified) external force is still needed to trigger the mechanochromic switches.[3d] The second is the crystallization of solid molecules.[4] Without the need for chemical modifications, this approach is relatively convenient, but the crystallization of solid is constrained by numerous environmental and structural effects. A lot of effort will be taken in preparing the crystalline solid, thus complicating the strategy and limiting the application. Herein, we report an innovative approach for the covalent-bond-activated mechanoresponsive molecules. The approach is characterized by noncovalent chemical modification, low external force (0.7 kg for rhodamine-β cyclodextrin (**Rh-βCD**), 2.2 kg for spiropyran-β cyclodextrin (**SP-γCD**)) requirement, and convenient preparation.

Motivated by the previous findings that **CD** can act as a host to interact with guest molecules, we introduce **CD** as a matrix in our mechanochromic research. **CD** is well-known for its capability of forming complex inclusions with small molecules.[5] The hydroxyl groups of **CD** form strong hydrogen bonds to induce host–guest interactions to stabilize the inclusion complex.[5c,6] These excellent interactions are the basic elements for mechanochromism. These interactions, along with the easy strategy affording the inclusion, prompted us to use **CD** for the mechanochromic study. Herein, Rh and SP were used as model fluorophores to form supramolecular complexes with **CD**s (**Scheme 1**). These two series of molecules are both outstanding environment-sensitive materials that have weak chemical bonds and undergo ring-opening procedures under different stimuli.[7] In particular,

---

S. Wan, Prof. F. Wang, Prof. W. Yang, Prof. M. Yin
State Key Laboratory of Chemical Resource Engineering
Key Laboratory of Carbon Fiber and Functional
Polymers of Ministry of Education
Beijing Laboratory of Biomedical Materials
Beijing University of Chemical Technology
Beijing 100029, P. R. China
E-mail: yinmz@mail.buct.edu.cn

Z. Ma, Prof. X. Jia
College of Chemistry and Molecular Engineering
Peking University
Beijing 100871, P. R. China

C. Chen, Prof. F. Li
State Key Laboratory of Superhard Materials
Jilin University
Jilin 130012, P. R. China

DOI: 10.1002/adfm.201504048

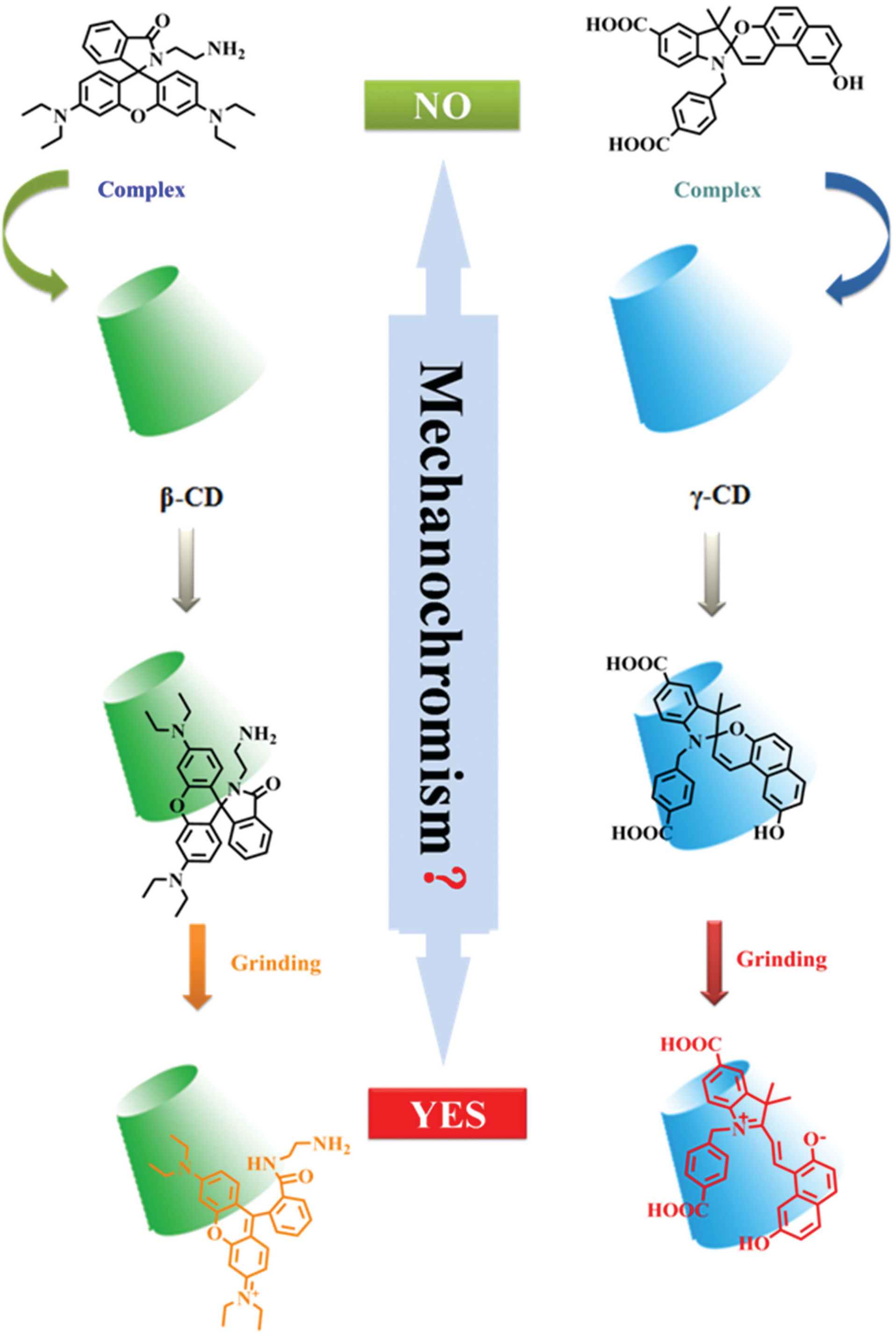

Scheme 1. Supramolecular complex of both **Rh** and **SP** with cyclodextrin toward mechanochromism.

the derivatives of these two fluorophores are considered as successful examples for realizing mechanochromism by either covalent chemical modifications or solid crystallizations.[3c,e] In this study, the two model fluorophore molecules initially could not reach their opening isomers upon shearing under a force of 10 kg. The mechanochromism was easily realized for both model molecules with little external forces (0.7 kg for **Rh-*β*CD**, 2.2 kg for **SP-*γ*CD**) by jacketing **CDs**. The strategy is easily achievable, and the small guest molecules can be readily replaced by other chromophore compounds with weak chemical bonds. In this way, the mechanochromic materials will match with more molecules, enduing them with easier writing and erasing properties by reducing their external force requirements and then facilitating the mechanochromic switches.

2. Results and Discussion

2.1. Synthesis and Characterization of CD Complex Inclusions

The selected Rh was synthesized according to a method given in the literature.[3b] Extremely stable SP was synthesized and discussed in our previous work.[7a] This SP was proved to be a good pH sensor and could not undergo ring-opening procedure unless under strong external stimuli. They were specially selected by guaranteeing that they cannot change colors upon heavy shearing (10 kg). The complex inclusions **Rh-βCD** and **SP-γCD** were conducted and confirmed by nuclear magnetic resonance spectroscopy (**NMR**), mass spectrometry (**MS**), Fourier transform infrared spectroscopy (**FTIR**), thermogravimetric analysis (**TGA**), and X-ray diffraction (**XRD**). Detailed structural characterizations are presented in Figures S1–S10 in the Supporting Information. Particularly, **γCD** was chosen as the **SP** inclusion matrix because **βCD** cannot fit **SP** very well. As shown in Figure S5 and S7 in the Supporting Information, the ^{1}H-NMR spectrum of **SP-βCD** presents no characteristic peak for **SP**, and the peak of **SP-βCD** in the electrospray ionization-time of flight mass spectrometry (ESI-TOF) spectrum is quite weak, indicating that **SP** and **βCD** can hardly form a complex. Only a tiny part of **SP** can be involved in the cavity of **βCD**, and **SP** can be washed out with acetone (Figure S11, Supporting Information). In other words, **SP** matches better with **γCD** than with **βCD**.

2.2. Supramolecule Mechanochromism in Film State

Because the molecules are more orderly arrayed in the film state than in the initial powder state, the samples of complex inclusions were fabricated into films on a quartz plate. Two methods can be used: One method is to dissolve the complex inclusions in dimethyl sulphoxide (DMSO) or *N*,*N*-dimethylformamide (DMF), and the solution is then dropped on the quartz plate and dried at 40 °C under vacuum overnight to form a thin film on the quartz plate (**Figure 1**A). The other method is to physically mix **SP** or **Rh** powder with **CD** powder, the mixture is dissolved in DMSO or DMF, and the solution is dropped on the quartz plate and then dried at 40 °C under vacuum overnight to afford the film state sample (Figure 1B). In order to achieve good mechanochromic performance, the sample needs to be rigidly dried. The grinding of the film state samples was performed in auto-grinding equipment (Figure S12, Supporting Information).

As expected, upon shearing of the film state samples, the complex inclusions of **Rh-βCD** and **SP-γCD** showed new colors, but neither of the isolated fluorophores did. Upon shearing, the color changed from nonfluorescence to orange for **Rh-βCD** (**Figure 2**A) and from nonfluorescence to reddish orange for **SP-γCD** (Figure 2B). By heating at 110 °C for several minutes (30 min for **Rh-βCD**) and (60 min for **SP-γCD**), these complex inclusions recovered to their original colors. Figure 2A,B shows the fluorescence changing of **Rh** and **SP** by grinding, for both the pre- and the postcomplex. These mechanochromic phenomena imply that **Rh-βCD** and **SP-γCD** are promising mechanochromic materials and inspire us to pursue further explorations.

To evaluate the effect on a quantitative level, we placed the film state samples in auto-grinding equipment (Figure S12, Supporting Information), which can grind the sample at a certain controllable force. In Figure 2C, the original emission band centered at 420 nm indicates a typical feature of the closed form of **Rh**.[8] Upon shearing under a force of 10 kg, no new peak is observed in the infrared region, indicating the absence of ring-opening procedure under this external stimulus. A similar phenomenon was observed in the mechanochromic test on **SP**. The emission band after grinding (10 kg) overlaps well with the original **SP** emission band, as shown in Figure 2E. The results in Figure 2C,E suggest that both of the isolated fluorophores **Rh** and **SP** cannot present mechanochromism properties even at a force of 10 kg before complexing. The superiority of the **CD** system was demonstrated by using it to jacket **Rh** and **SP**. The optical properties of **Rh-βCD** and **SP-γCD** change upon shearing. As shown in Figure 2D, for a film state sample of **Rh-βCD** ground at a force of only 0.7 kg, in addition to the emission peak at 420 nm for **Rh**, a new peak at around 578 nm appears. This new peak is attributed to the emergence of the ring-opening form of **Rh-βCD** (Figure S13A, Supporting

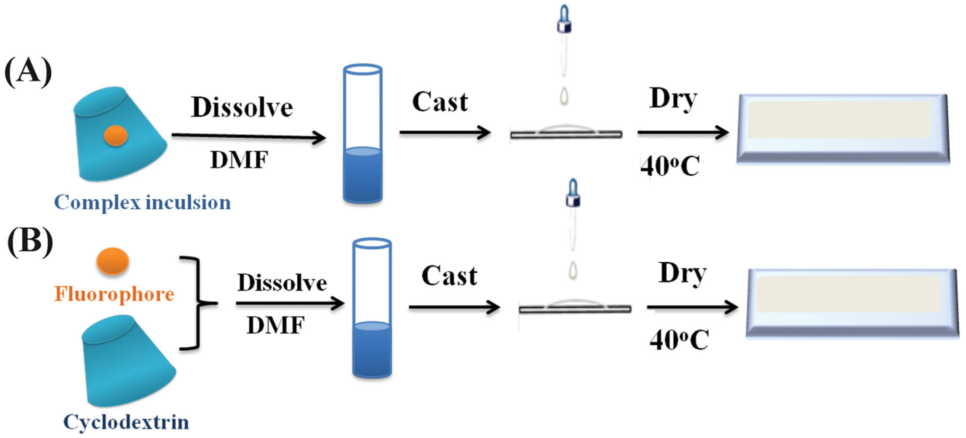

Figure 1. Two casting methods for preparation of film state samples: A) Complex inclusion **Rh-βCD** or **SP-γCD**; B) physically mixing **SP** or **Rh** with **CD** powder.

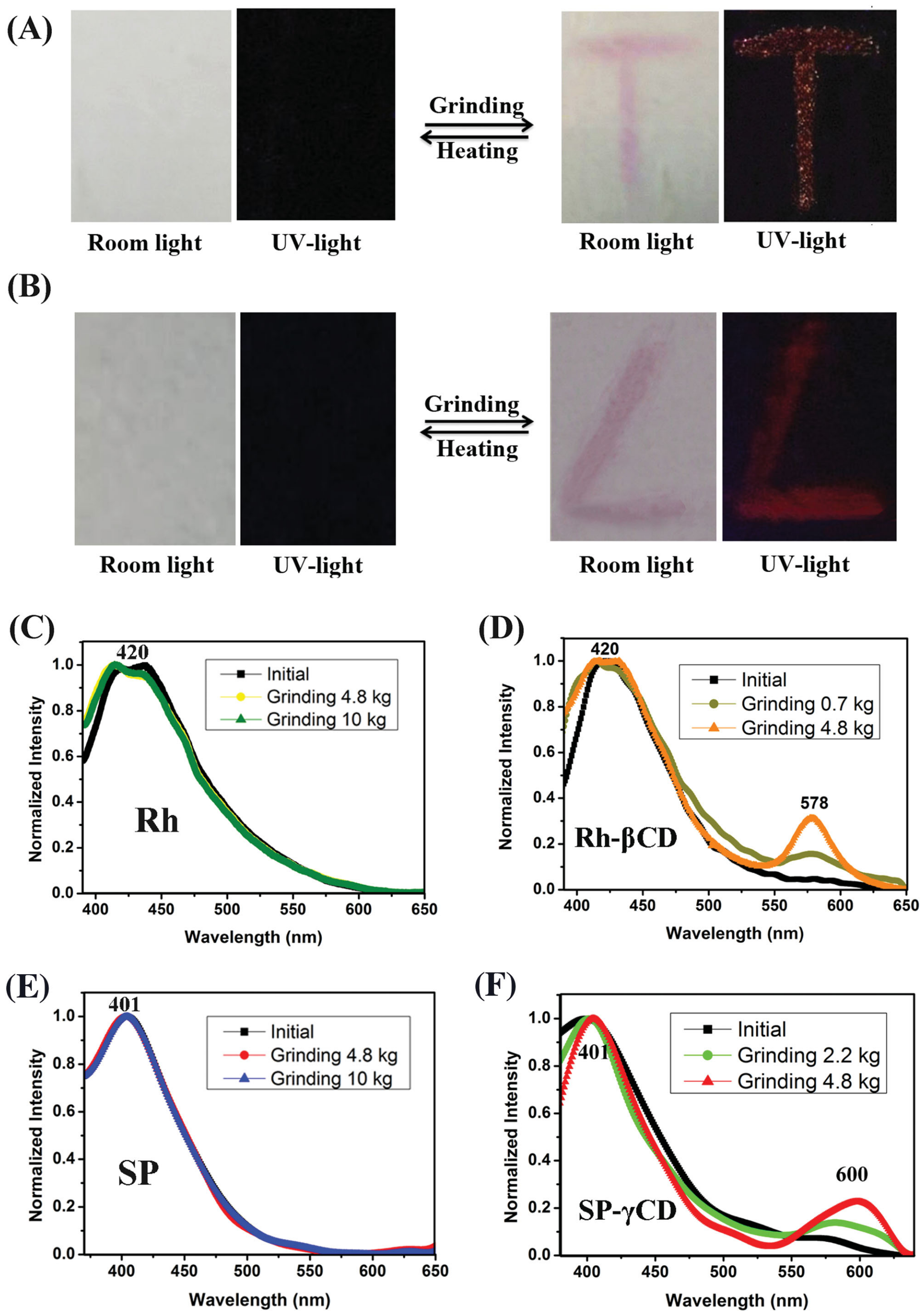

Figure 2. Mechanochromic test on quartz plate, with reversible color change under both room- and UV-light upon grinding and heating: A) **Rh-βCD** and B) **SP-γCD**. Fluorescence spectra of fluorophore film with and without grinding: C) **Rh**; D) **Rh-βCD**; E) **SP**; F) **SP-γCD**.

Information), and the intensity of this peak increases with the increase of external force.

This mechanochromic property was also observed for **SP-γCD**. As shown in Figure 2F, a new peak centered at about 600 nm, which belongs to the ring-opening form of SP **SP-γCD** (Figure S13B, Supporting Information), begins to appear at a force of 2.2 kg, and the fluorescence intensity increases with the increase of external force. In addition, for both **Rh-βCD** and **SP-γCD**, the mechanochromic switches can be repeated for at least five times by grinding and heating (Figure S14, Supporting Information). These results show that the jacketing of **SP** or **Rh** molecules with **CD** can minimize the required external force for triggering the mechanochromic switches. Therefore, an innovative and convenient way has been developed to achieve an effective mechanochromic switch that applies to both **Rh** and **SP**, by complexing with **CD**s.

2.3. Supramolecule Mechanochromism in Powder State

To study the supramolecule effects on the mechanochromism of **SP** and **Rh** in the powder state, we put the powder samples in diamond anvil cell equipment, which can generate hydrostatic pressures with dozens of gigapascals at room temperature (Figure S15, Supporting Information).[9] As shown in **Figure 3**A,C, when the pressure is gradually focused on **Rh** and **Rh-*β*CD**, their fluorescent spectra change in different ways. For the initial **Rh** powder, there exists little open form, which presents a weak fluorescent signal between 500 and 600 nm. When the external pressure is gradually increased, the fluorescent intensity of **Rh** centered at 580 nm continuously decreases, broadens, and redshifts. This fluorescence change phenomenon is attributed to the assembly of **Rh** molecules. Thus, the fluorescence was quenched by the aggregation-caused quenching (**ACQ**) effect.[10] This result indicates that during the focusing of external pressure, none or very little open form is generated. In other words, the isolated **Rh** molecules hardly perform mechanochromism. Once **Rh** is jacketed with ***β*CD**, the discipline changes. As the external pressure is focused and gradually increased on the **Rh-*β*CD** powder, the fluorescent intensity of the **Rh-*β*CD** powder at 560 nm continuously increases until the pressure reaches 1.79 GPa. Therefore, in the pressure range 0 to 1.79 GPa, the open form of **Rh-*β*CD** generated by pressure gains the support of the **ACQ** effect. In the pressure range 2.46 to 9.88 GPa, the fluorescent intensity of **Rh-*β*CD** at 560 nm decreases, broadens, and redshifts. As the pressure continues to increase (11.84–18.36 GPa), the intensity of fluorescence belonging to the open form of **Rh** increases again. According to the results of the above pressure tests, the supramolecule effect facilitates the triggering of the mechanochromic switch of **Rh**. This effect was also applied to the **SP** system. Similar pressure tests on **SP** and **SP-*γ*CD** were performed (Figure 3B,D). For the **SP** powder, as the pressure is gradually increased, the fluorescence intensity at 625 nm continuously decreases. But for **SP-*γ*CD**, the fluorescence intensities at 600 nm continuously increase in the pressure range 0 to 9.97 GPa, suggesting that a relatively large amount of open form is generated and that the jacketing of **CD** also facilitates the mechanochromism of **SP**.

The supramolecular mechanochromic system was investigated on one isolated complex inclusion scale first to determine the role of microscale host–guest interaction. Because of the presence of hydrogen bonds in **CD**, the specific binding sites between **CD** and the fluorophores need to be analyzed. Thus, the geometric conformations of these two complex systems were calculated with Gaussian 09. The molecular sizes of **Rh**

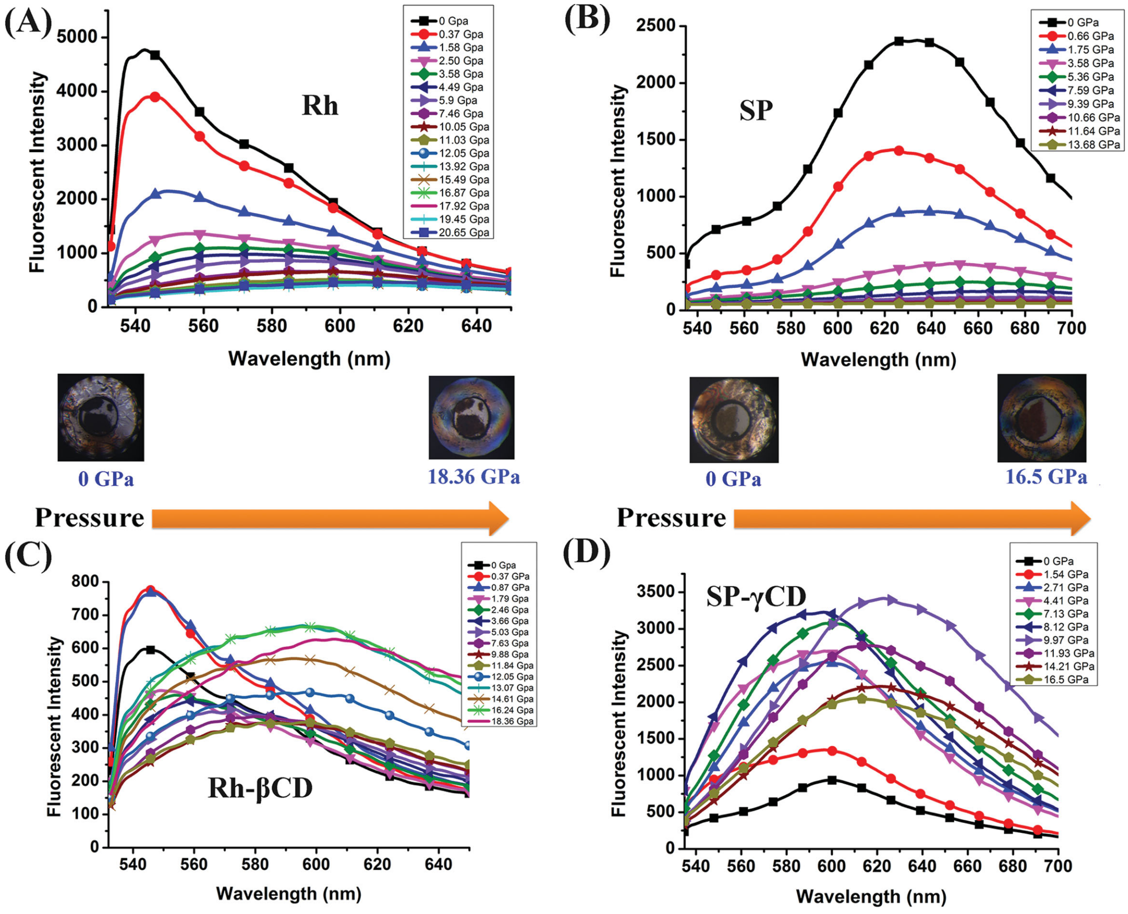

Figure 3. Variations of in situ fluorescent spectra of fluorophore powder in diamond anvil cell (**DAC**) equipment with pressure: A) **Rh**; B) **SP**; C) **Rh-*β*CD**; D) **SP-*γ*CD**.

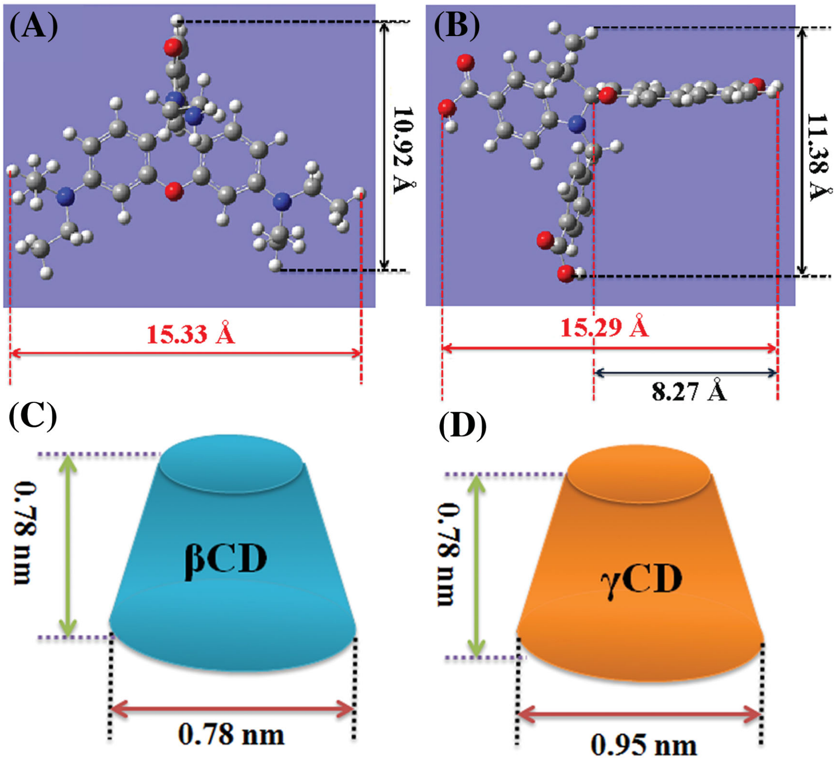

Figure 4. Geometric conformations of A) **Rh**; B) **SP**; C) ***β*****CD,** and D) ***γ*****CD**.

and **SP** are shown in the **Figure** 4A,B, respectively. The heights of ***β*****-CD** and ***γ*****-CD** are about 7.8 Å (Figure 4C,D).[11] The lengths of **Rh** and **SP** were calculated to be 15.33 and 15.29 Å, respectively, and the widths, 10.91 and 11.38 Å, respectively. The geometric conformations of **Rh** and **SP** are much larger than those of ***β*****-CD** and ***γ*****-CD**, indicating that both **Rh** and **SP** are partly included in the **CD** cavities. Accurate and intuitive space-filling molecular models of **Rh-*β*CD** and **SP-*γ*CD** complex are presented in **Figure 5**. The approximate lowest energy was estimated with Autodock 4.0.[12] The results show that **Rh** and **SP** can be well included in ***β*****CD** and ***γ*****CD**, respectively. Moreover, the groups including COOH, OH, and NH_2 are close to the OH groups of the **CD**s, making it easy to form hydrogen bonds.

Generally, when guest molecules are incorporated in the **CD** cavity, the **XRD** patterns of these complexes should be clearly distinct from those obtained by the superimposition of the pattern of each component.[5d] The **XRD** results of **Rh**, ***β*****CD**, the physical mixture of **Rh** and ***β*****CD** (1:1, mol/mol), and the complex inclusion are shown in **Figure** 6A. It is clear that the diffractogram of the inclusion complex is different from the pattern of the physical mixture, which is the superposition of the individual patterns of **Rh** and ***β*****CD**. A similar phenomenon is observed in the **XRD** results of **SP**, ***γ*****CD**, the physical mixture of **SP**, and ***γ*****CD** (1:1, mol/mol), and **SP-*γ*CD** (Figure 6B). Moreover, similar results are observed in the **TGA**, **FTIR**, and derivative thermogravimetric analysis (**DTG**) results, further confirming the formations of complex inclusions. The types of complex inclusions were confirmed by electrospray ionization mass spectrometry and matrix-assisted laser desorption/ionization time of flight mass spectrometry (**MALDI-TOF-MS**).[13] The peaks observed at m/z 900 (double charge) and 1803 for **SP-*γ*CD** (Figure 6C) indicate one fluorophore in one fluorophore-**CD** complex inclusion.

Rotating-frame Overhauser-effect spectroscopy (**ROESY**) was used to verify the geometric position of the fluorophore in the **CD** cavity in the complex (**Figure** 7; Figure S16, Supporting Information).[5b] The **ROESY** spectrum of an equimolar complex of ***β*****CD** and guest **Rh** molecules display clear nuclear Overhauser-effect (**NOE**) correlations between the H-2 protons of ***β*****CD** and the methyl protons of the diethylamino groups in **Rh**, and the **NOE** correlation between the H-4 protons of ***β*****CD** and the bottom aromatic protons of **Rh**, suggesting the formation of **Rh-*β*CD** complex inclusion. The **ROESY** spectrum of **SP-*γ*CD** displays three main clear **NOE** correlations. The first is the

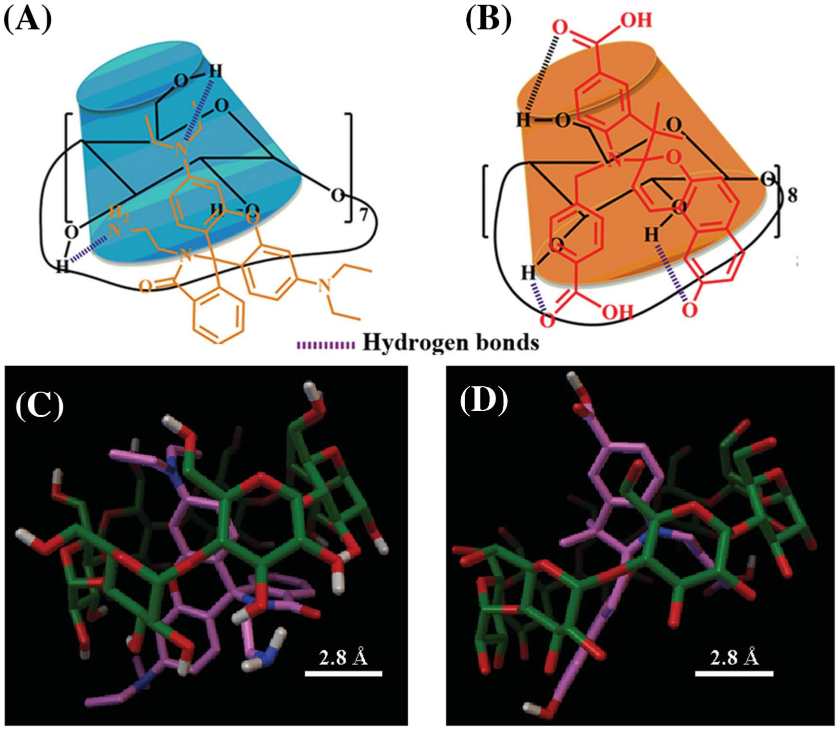

Figure 5. Probable hydrogen bonds connecting A) ***β*****CD** with **Rh** and B) ***γ*****CD** with **SP**; Space-filling molecular models of 3D conformations of C) **Rh-*β*CD** and D) **SP-Γcd**.

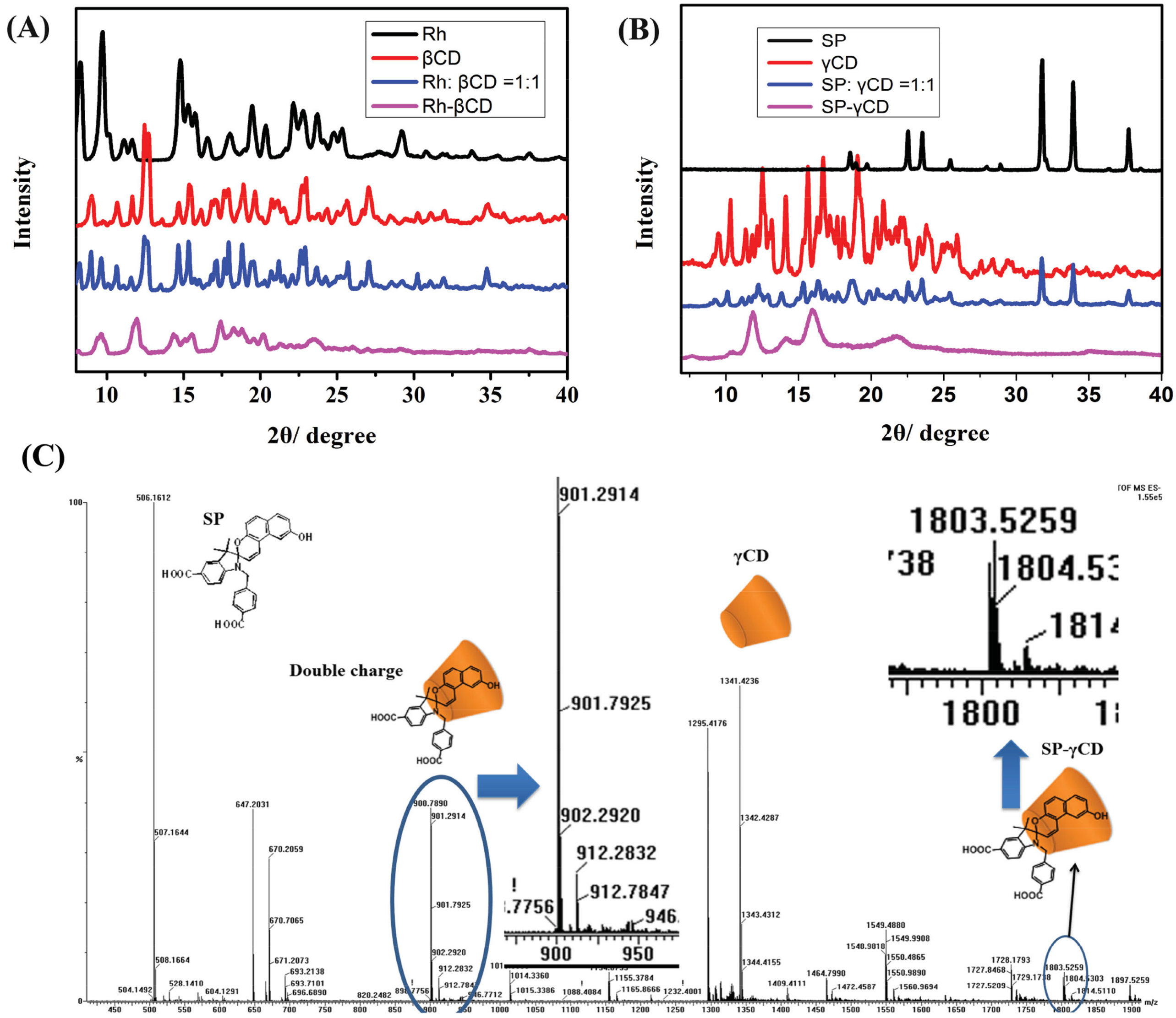

Figure 6. XRD comparison of A) **Rh**, ***β*****CD**, **Rh**/ ***β*****CD** mix = 1:1, **Rh-*β*CD**, B) **SP**, ***γ*****CD**, **SP**/ ***γ*****CD** mix = 1:1, **SP-*γ*CD**; C) **ESI-TOF** of **SP-*γ*CD**.

correlation between the H-1 protons of ***γ*****CD** and the aromatic protons on the N-position of the indole part, the second is the correlation between OH-3 and the aromatic protons on naphthalene, and the third is the correlation between H-2 of ***γ*****CD** and the phenolic hydroxyl of **SP**. These three **NOE** signals also suggest a true formation of **SP-*γ*CD** complex inclusion. These correlations present the conformations of **Rh-*β*CD** and **SP-*γ*CD**, and the results are well consistent with the calculation conformations shown in Figure 5. Moreover, the phenolic hydroxyl signal indicates the formation of hydrogen bonds between **CD** and **SP**. According to these results, **Rh** or **SP** is accommodated in the cavity of **CD**, as shown in Scheme 1.

As reported in the literature,[2b,3e] structures with mechanochromic switch are generally well designed to induce intermolecular interactions. Thus, the mechanochromism in this supermolecular complex system may be due to the interactions between **CD** and the fluorophore. Generally, in **CD** inclusions, the molecules are locked by various forces such as hydrogen bonding, hydrophobic interaction, and van der Waals force.[8] To evaluate the effect of the leading factor on this supermolecular complex system, the thermodynamic parameters of interactions between **CD** and the fluorophore (**Rh**/***β*****CD** and **SP**/***γ*****CD**) were quantified by isothermal titration calorimetry (**ITC**). The acquired titration curves and thermodynamic parameters are shown in **Figure 8** and Figure S17 in the Supporting Information. As shown in Figure 8, ΔH and ΔS in this system are both negative with a measured affinity constant of $K_A = 1.099 \times 10^4\ \text{M}^{-1}$, indicating that the strong hydrogen bonds play a dominate role in the interaction of **SP**/***γ*****CD** as well.[14] Besides, similar results were observed for **Rh**/***β*****CD** interaction. As shown in Figure S17 in the Supporting Information, the negative ΔH, positive ΔS, and a high measured affinity constant (KA = $4.121 \times 10^4\ \text{M}^{-1}$) indicate that the strong hydrogen bonding accompanied by hydrophobic force is the leading factor for **Rh**/***β*****CD** interaction.[14] In Figure S10 in the Supporting Information, the peaks at about 3300 cm^{-1} in the **FTIR**

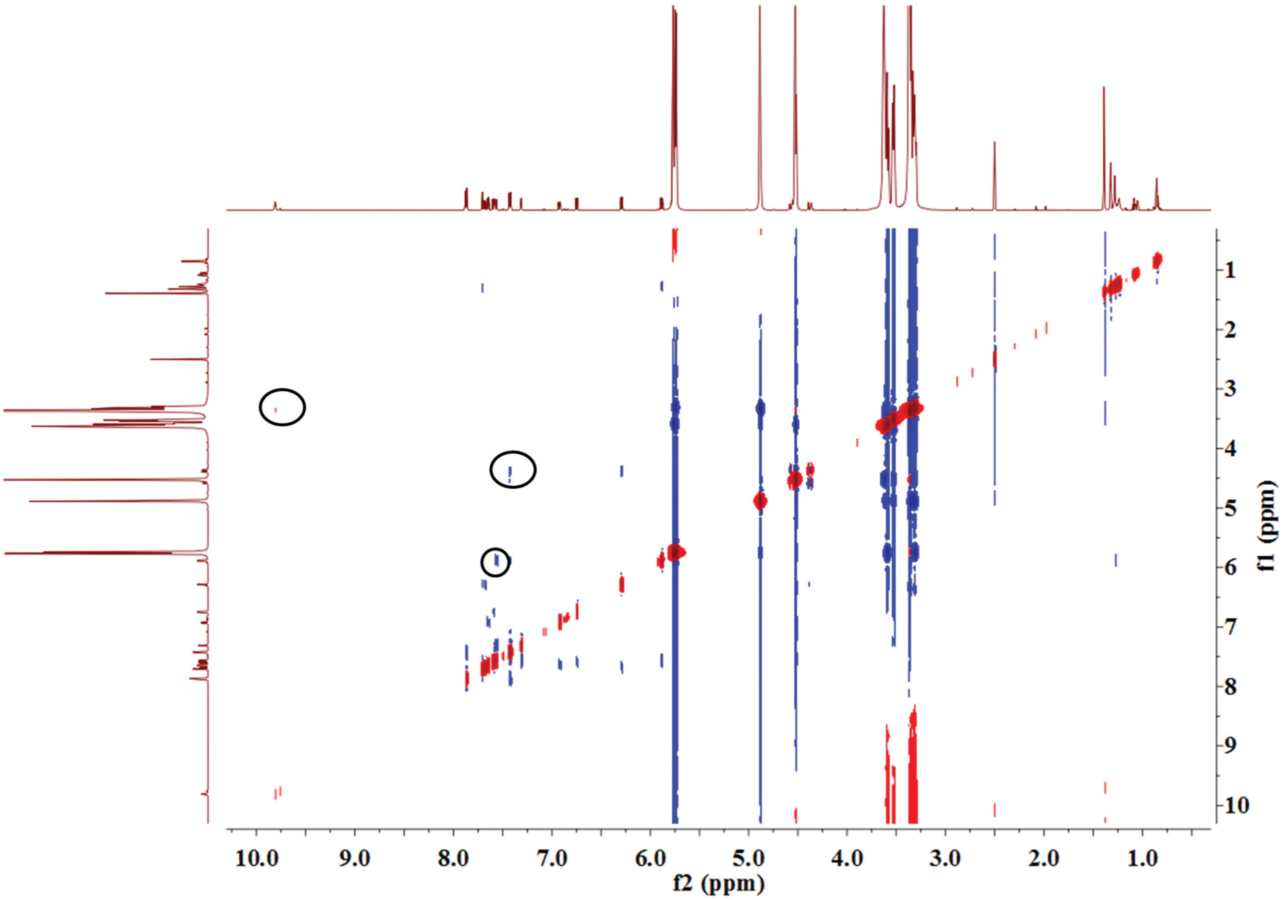

Figure 7. 2D NMR ROESY spectrum of **γCD** and **SP** complex.

spectra of both **Rh-βCD** and **SP-γCD** also suggest that strong hydrogen bonds exist in these two complex systems.[2b,15]

The function of hydrogen bond was initially explored by varying the temperature, which is a significant factor affecting the hydrogen bonds. With the temperature rising, the hydrogen bonds start to break. Therefore, we dropped and dried the samples (**Rh-βCD** and **SP-γCD**) on quartz plates at different temperatures to monitor the strengths of the hydrogen bonds. With the increase of temperature, the samples became harder to write. At temperatures above 130 °C, most of the hydrogen bonds broke, and the samples did not present obvious mechanochromism even upon shearing at a force of 5.6 kg. We supposed that the hydrogen bonds, which were provided by the stretching of **CD** to specific sites of the fluorophore, were involved in locking the fluorophore, thus triggering mechanochromism. Previous reports demonstrated that the force acting on both sides of weak chemical bonds can make the mechanochromism more achievable.[3c] The fluorophores **Rh** and **SP** do not have strong hydrogen bond providers and consequently cannot focus enough force on the weak chemical bonds of the fluorophores. By complexing **Rh** or **SP** with **CD**, numerous hydrogen bonds are formed. Besides, the hydrogen bonds prefer to complex with hetero atoms such as N and O that are readily found on both sides of the weak chemical bonds in **Rh** and **SP**. Considering the geometrical positions of **Rh** and **SP** in the **CD** complex system presented in Scheme 1 and Figure 5, the hydrogen bonds were simulated to stretch in the way as shown in Figure 5A,B. The hydrogen bonds provided by the large **CD** matrix seize both sides of the weak chemical bonds inside the fluorophore and then tightly lock the fluorophore, strengthening the interactions in one single complex inclusion. In this way, the external force is easily focused on the weak chemical bonds upon shearing, thus triggering the mechanochromic switches.

To ensure the essential role of microscale host–guest interactions in facilitating the mechanochromism, we introduced different types of **CD** to complex with **Rh** and **SP**. Based on the geometric conformations of **Rh**, **SP**, and different types of **CDs** (Figure 5; Figures S11 and S18, Supporting Information) and the above experimental data, **Rh** is best suited to **βCD** and is partly involved in **αCD**. **SP** is best suited to **γCD**, worst suited to **αCD**, and is partly involved in **βCD**. We compared the mechanochromic performances of different complex inclusions including **Rh-α/βCD** and **SP-α/β/γCD** by the quantitative grinding tests. The samples were prepared according to the second method in Figure 1B. For **Rh-αCD**, the fluorescent spectrum belonging to its open form can be observed only upon grinding at a force of 2.3 kg, much higher than the force of 0.7 kg for **Rh-βCD** (Figure S19A, Supporting Information). For **SP-βCD**, the fluorescent spectrum belonging to its open form is generated upon grinding at a force of 5.2 kg, also much higher than the force of 2.2 kg for **SP-γCD** (Figure S19C, Supporting

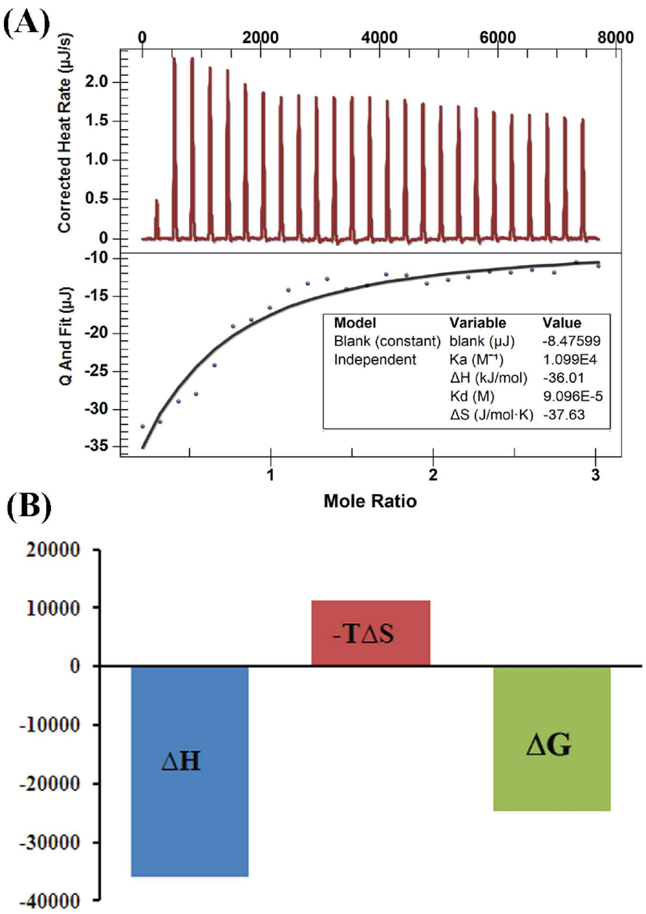

Figure 8. A) Heat effects measured by **ITC** in the titration of aqueous solutions of **SP** with **γCD**; B) Thermodynamic parameters of the interactions of **SP** and **γCD**.

Information). For **SP-αCD**, even upon grinding at a force of 5.6 kg, no mechanochromism was observed (Figure S19B, Supporting Information). Therefore, the host–guest complexation between the fluorophore and **CD** matches better, and the required external force for triggering the mechanochromic switches is lower. In addition, the **Rh** or **SP** was simply dispersed in the H-bond to form polymer matrices like polyvinylalcohol, and then the mixtures were dropped on the plate and dried overnight under vacuum. No mechanochromism were observed after shearing these samples (Figure S20, Supporting Information). These conclusions further support the effect of microscale host–guest interaction of **CD** on the mechanochromism.

2.4. Macroscale Aggregations

During the mechanochromic tests, we found that the film state samples of **Rh-βCD** and **SP-γCD** trigger the mechanochromic switches much more easily than the powder state samples. Therefore, we suspect that the macroscale aggregations caused by hydrogen bonding also play a role in facilitating the mechanochromism. DMF and DMSO are solvents that can break hydrogen bonds and the macroscale aggregations of **Rh-βCD** and **SP-γCD**. During the preparations of film state samples, the initial powder samples were dissolved in DMF or DMSO and dried. For the samples to be totally dried, the drying procedure needs to last for more than 6 h. According to these disciplines, we prepared a film state sample that can dry in less than 2 h. This sample has a little residual DMF/DMSO, which can break the hydrogen bonds and in turn change the macroscale aggregations. Therefore, we compared the mechanochromic-related differences between samples dried for 2 and 6 h to explore and determine the effect of macroscale aggregations on mechanochromism. In the quantitative mechanochromic test on **Rh-βCD** and **SP-γCD**, the samples of **Rh-βCD** dried for 2 and 6 h exhibit mechanochromism behavior under forces of 2.3 and 0.7 kg, respectively. For **SP-γCD**, the samples dried for 2 and 6 h show mechanochromism under forces of 4.7 and 2.2 kg, respectively. These results confirm that it is much harder for the samples dried for 2 h than for the samples dried for 6 h to perform mechanochromism, for both **Rh-βCD** and **SP-γCD**. Therefore, as we suspected, the macroscale aggregations caused by hydrogen bonding also play a role in this system. The residual DMF/DMSO in the sample dried for 2 h breaks the hydrogen bonds, and the macroscale aggregations of **Rh-βCD** and **SP-γCD** make it harder for these complexes to trigger the mechanochromic switches.

To visually explore the function of hydrogen bonds in macroscale aggregations between the complex inclusions, we designed a way to break the hydrogen bonds in the **CD** complex inclusions by the addition of NaOH. The three types of hydroxyl groups in **CD** are slightly acidic, especially the 2-position hydroxyl groups.[16] The addition of NaOH increases the pH of the complex and turns these three types of hydroxyl groups into sodium salts (**Figure 9**A), and in turn destroys most of the hydrogen bonds. Once the hydrogen bonds are involved in particle aggregation, the morphology of the **CD** complex particles will change with the addition of NaOH (Figure 9B). This variation was confirmed by scanning electron microscope (SEM) imaging. Figure 9 shows the morphology variations of **Rh-βCD** and **SP-γCD** with the addition of NaOH. The original morphology of **Rh-βCD** or **SP-γCD** is that of an ordered continuous substance (Figure 9C,E), indicating large scale aggregations of the complex inclusions. After the addition of NaOH, this ordered continuous substance breaks into scattered spot adjuncts (Figure 9D,F). These changes suggest a crucial role of hydrogen bonds in gathering the isolated complex inclusions. And these scattered spot adjuncts show almost no mechanochromic behavior. In conclusion, the hydrogen bonds not only participate in one complex inclusion, but also prompt the aggregations of **CD** complex inclusions. These ordered, large-scale aggregations strengthen the molecular interactions, which in turn facilitate the transfer of external force. In this way, the force can easily pass on to the next complex inclusion, thus triggering the mechanochromic switches.

In the constrained optimization approach, the effect of an applied force is modeled by optimizing the molecular geometry subject to a distance constraint between two atoms.[3c] In this study, the constrained geometries simulate external force (**COGEF**) method was employed to establish the mechanochromic models.[17] Related mechanochromic calculations on Rh were reported previously.[3e] As shown in **Figure 10**,

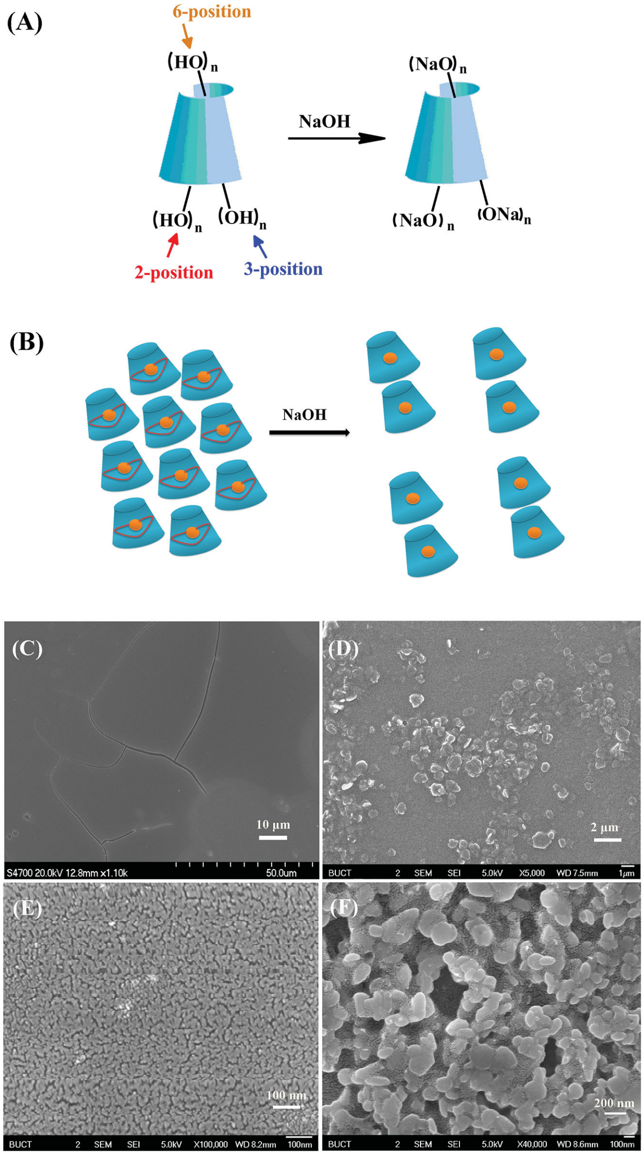

Figure 9. A) The variation in one complex particle after the addition of NaOH; B) The variation between complex particles after the addition of NaOH. **SEM** images of **Rh-βCD** C) before and D) after the addition of NaOH; SEM images of **SP-γCD** E) before and F) after the addition of NaOH ($C = 5 \times 10^{-4}$ M).

bond 1 is a relatively weak bond in the **SP** molecule. The **SP** model was built by simulating the cleavage of bond 1 and calculating the activation energy of fragmentation with **COGEF**. When bond 1 is gradually stretched from 1.43 Å to the breaking point of 1.52 Å, the activation energy increases from 2.43 to 7.15 kJ mol^{-1}. Thus, the average minimum external force required to induce the breaking of bond 1 of **SP** is 2.41 nN.

On the basis of the above results and analyses, a mechanism for the mechanochromic switch of this supramolecular system can be proposed. In one complex particle, **CD** can provide strong hydrogen bonds to seize both sides of the chemical bonds of the fluorophores and tightly lock the fluorophores. Hydrogen bonds prompt the aggregation of complex inclusions in large ordered arrays among the complex particles, thus strengthening the interactions between molecules. The isolated uncomplexed small molecules of **Rh** and **SP** can focus only low external forces on the weak chemical bonds upon shearing, which are far from enough to induce bond breakage. By complexing **Rh** or **SP** with the host **CD**, these two supramolecular systems were built through hydrogen bonds. With the hydrogen bonds, the external forces can effectively pass to both sides of the weak chemical bonds of the fluorophores to make the bonds stretch more easily upon shearing, and mechanochromism is achieved.

3. Conclusion

Supramolecular mechanochromism was successfully realized by jacketing the host **CD** with the guest **Rh** or **SP** molecules. This innovative and convenient strategy can make some fluorophores achieve mechanochromism and thus both easy writing and erasing effects. The strong hydrogen bonds provided by **CD** play a crucial role in these supramolecular mechanochromic systems. Because both sides of the weak chemical bonds in the **Rh** or **SP** fluorophores are seized and locked by the hydrogen bonds, and the ordered aggregation of complex particles caused by the hydrogen bonds enhances the interactions, the weak chemical bonds can focus more external force and stretch more easily upon shearing. To the best of our knowledge, this report is the first to correlate a mechanochromic reaction with a supramolecular system. The two supramolecular mechanochromic systems gain an edge over other reported mechanochromic materials for providing not only the noncovalent chemical modification, low external force requirement (0.7 kg for **Rh-βCD**, 2.2 kg for **SP-γCD**), and convenient preparation, but also the mechanochromic switches on diverse fluorophores with only one strategy and facile preparation, and are of great importance in practical applications.

4. Experimental Section

^{1}H/2D and ^{13}C-NMR spectra were recorded on a Bruker 400 (400 MHz ^{1}H; 100 MHz ^{13}C) or Bruker 600 (600 MHz ^{1}H; 150 MHz ^{13}C) spectrometer at room temperature. Mass spectra (MS) were measured with a XEVO-G2QTOF (ESI) (Waters, USA). Fluorescence spectroscopic studies were performed on a fluorescence spectrophotometer (Horiba Jobin Yvon FluoroMax-4 NIR, NJ, USA). Powder XRD patterns were carried out on a D/max2500 VB2+/PC X-ray diffractometer (Rigaku) using Cu Kα radiation in the 2θ range 5°–40°. FTIR spectra (KBr pellets) were recorded on a NEXUS 670 FTIR spectrometer (Nicolet, US). Nano ITC (TA Instruments Waters, LLC, UT) was used for ITC experiments. TGA was recorded on (TA Instruments Waters, USA). MALDI-TOF MS were performed on Bruker Daltonics Inc. BIFLEXIII MALDI-TOF mass spectrometer.

Scanning Electron Microscope (SEM): SEM observation was recorded on HITACHI S-4700 (Japan) SEM at an accelerating voltage of 10 kV. Samples ($C = 5 \times 10^{-4}$ M, $T = 298.15$ K) were vacuum sputtered with Pt before SEM observation.

Synthesis of Rh: After Rh B (1g, 2 mmol) was dissolved in ethanol (10 ml), ethylenediamine (2 mL) was added dropwise into the mixture and reflux for 12 h. Ethanol was then evaporated under vacuum. The residual mixture was dropped into water. After extracting with

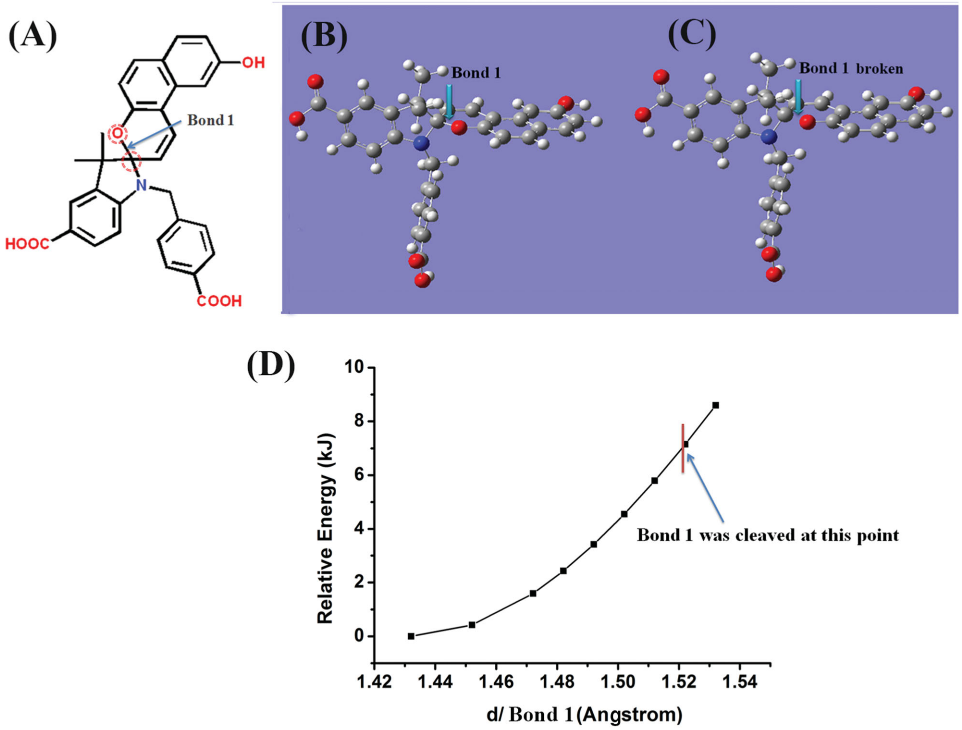

Figure 10. A) Chemical structure of **SP** used in calculation (the distance of Bond 1 increased gradually with the simulation time, B) initial optimized **SP** structure, C) optimized **SP** structure when Bond 1 was broken, and D) variation of energy of **SP** with extensions of bond 1.

dichloromethane for three times, the organic layer was collected and then evaporated under vacuum, crude product was further purified through a short silica gel eluting with ethyl acetate to afford **Rh** as a light pink solid (0. 66 g, yield 75%). ^{1}H NMR (400 MHz, $CDCl_3$) δ 7.89 (dt, *J* = 7.5, 3.3 Hz, 1H), 7.48–7.40 (m, 2H), 7.12–7.06 (m, 1H), 6.43 (*d*, *J* = 8.8 Hz, 2H), 6.37 (*d*, *J* = 2.5 Hz, 2H), 6.28 (*d*, *J* = 2.6 Hz,1H), 6.26 (*d*, *J* = 2.6 Hz, 1H), 3.33 (*q*, *J* = 7.1 Hz, 8H), 3.21 (*t*, *J* = 6.2 Hz, 2H), 2.51 (*t*, *J* = 6.2 Hz, 2H), 2.44–2.12 (m, 2H), 1.16 (*t*, *J* = 7.0 Hz, 12H). ^{13}C NMR (101 MHz, $CDCl_3$) δ 168.61, 153.50, 153.29, 148.82, 132.38, 131.27, 128.70, 128.03, 123.83, 122.76, 108.16, 105.70, 97.73, 64.92, 44.35, 43.91, and 40.87. ESI-TOF: *m*/*z* calcd for $C_{30}H_{37}N_4O_2$, 485.2816; found, 485.2921 (M+H$^+$).

*Preparation of CD Complex Inclusions **Rh-βCD***: After **βCD** (113.5 mg, 0.1 mmol) was dissolved in warm water (50 °C) until their gain saturate, a solution of **Rh** (50 mg, 0.1 mmol) in ethanol (2 mL) was added dropwise into the **βCD** aqueous solution. The suspension was vigorous stirred at 40 °C for 5 h. Solvent was then evaporated under vacuum. The residue solid was washed with little cold water and acetone, and then dried at room temperature in vacuo to afford a white complex **Rh-βCD.**

SP-βCD: After **βCD** (1.135 g, 1 mmol) was dissolved in the mixture of water (20 ml) and ethanol (2 ml) at 40 °C, a solution of **SP** (50 mg, 0.1 mmol) in ethanol (2 mL) was added dropwise into the **βCD** solution. The suspension was vigorous stirred at 40 °C for 5 h. The mixture was then kept at 4 °C for 20 h. The obtained precipitate was filtered out, washed with water and acetone, and dried at room temperature in vacuo to afford a light pink complex **SP-βCD**.

SP-γCD: After **γCD** (1.135 g, 1 mmol) was dissolved in the mixture of water (20 ml) and ethanol (2 ml), a solution of **SP** (50 mg, 0.1 mmol) in ethanol (2 mL) was added dropwise into the **γCD** solution. The suspension was vigorous stirred at room temperature for 5 h. The mixture was then kept at 4 °C for 20 h. The obtained precipitate was filtered out, washed three times with 5 mL of cold water–ethanol (40% v/v), and dried at room temperature in vacuo to afford a yellow complex **SP-γCD**.

Supporting Information

Supporting Information is available from the Wiley Online Library or from the author.

Acknowledgements

This work was financially supported by the National Natural Science Foundation of China (Grant Nos. 21174012, 51221002, and 21574009), the Beijing Natural Science Foundation (Grant No. 2142026), and the Innovation and Promotion Project of Beijing University of Chemical Technology.

Received: September 23, 2015
Revised: October 25, 2015

---

[1] a) Z. Chi, X. Zhang, B. Xu, X. Zhou, C. Ma, Y. Zhang, S. Liu, J. Xu, *Chem. Soc. Rev.* **2012**, *41*, 3878; b) Y. Sagara, T. Kato, *Angew. Chem.* **2011**, *123*, 9294; c) Y. Sagara, T. Kato, *Nat. Chem.* **2009**, *1*, 605; d) M. S. Kwon, J. Gierschner, S. J. Yoon, S. Y. Park, *Adv. Mater.* **2012**, *24*, 5487; e) X. Zheng, X. Wang, H. Mao, W. Wu, B. Liu, X. Jiang, *Nat. Commun.* **2015**, *6*, 5834; f) M. Chen, M. Yin, *Prog. Polym. Sci.* **2014**, *39*, 365; g) Q. Qi, J. Qian, X. Tan, J. Zhang, L. Wang, B. Xu, B. Zou, W. Tian, *Adv. Funct. Mater.* **2015**, *25*, 4005.

[2] a) G. Zhang, J. Lu, M. Sabat, C. L. Fraser, *J. Am. Chem. Soc.* **2010**, *132*, 2160; b) M. Teng, X. Jia, X. Chen, Z. Ma, Y. Wei, *Chem. Commun.* **2011**, *47*, 6078; c) M. J. Teng, X. R. Jia, S. Yang, X. F. Chen, Y. Wei, *Adv. Mater.* **2012**, *24*, 1255; d) J. Kunzelman, M. Kinami, B. R. Crenshaw, J. D. Protasiewicz, C. Weder, *Adv. Mater.* **2008**, *20*,

119; e) B. R. Crenshaw, C. Weder, *Chem. Mater.* **2003**, *15*, 4717; f) F. Ciardelli, G. Ruggeri, A. Pucci, *Chem. Soc. Rev.* **2013**, *42*, 857.
[3] a) S. L. Potisek, D. A. Davis, N. R. Sottos, S. R. White, J. S. Moore, *J. Am. Chem. Soc.* **2007**, *129*, 13808; b) Y. Chen, H. Zhang, X. Fang, Y. Lin, Y. Xu, W. Weng, *ACS Macro Lett.* **2014**, *3*, 141; c) D. A. Davis, A. Hamilton, J. Yang, L. D. Cremar, D. Van Gough, S. L. Potisek, M. T. Ong, P. V. Braun, T. J. Martínez, S. R. White, *Nature* **2009**, *459*, 68; d) Z. Ma, M. Teng, Z. Wang, S. Yang, X. Jia, *Angew. Chem. Int. Ed.* **2013**, *52*, 12268; e) Y. Chen, A. Spiering, S. Karthikeyan, G. W. Peters, E. Meijer, R. P. Sijbesma, *Nat. Chem.* **2012**, *4*, 559; f) C. M. Degen, P. A. May, J. S. Moore, S. R. White, N. R. Sottos, *Macromolecules* **2013**, *46*, 8917.
[4] D. Tipikin, *Russ. J. Phys. Chem.* **2001**, *75*, 1720.
[5] a) R. Li, C. S. Santos, T. B. Norsten, K. Morimitsu, C. Bohne, *Chem. Commun.* **2010**, *46*, 1941; b) B. Lv, Z. Wu, C. Ji, W. Yang, D. Yan, M. Yin, *J. Mater. Chem. C* **2015**, *3*, 8519; c) J. Szejtli, *Chem. Rev.* **1998**, *98*, 1743; d) S. Zhang, M. Fan, Y. Liu, Y. Ma, G. Zhang, J. Yao, *Langmuir* **2007**, *23*, 9443; e) J. A. Ferreira, S. Costa, *J. Photochem. Photobiol. A.* **2005**, *173*, 309; f) S. Yu, Y. Zhang, X. Wang, X. Zhen, Z. Zhang, W. Wu, X. Jiang, *Angew. Chem. Int. Ed.* **2013**, *52*, 7272.
[6] L.-F. Wang, J.-W. Chen, J.-W. Chen, *Mater. Chem. Phys.* **2012**, *136*, 151.
[7] a) S. Wan, Y. Zheng, J. Shen, W. Yang, M. Yin, *ACS Appl. Mater. Inter.* **2014**, *6*, 19515; b) R. Klajn, *Chem. Soc. Rev.* **2013**, *43*, 148; c) X. Zhou, X. Wu, J. Yoon, *Chem. Commun.* **2015**, *51*, 111; d) N. Shao, J. Jin, H. Wang, J. Zheng, R. Yang, W. Chan, Z. Abliz, *J. Am. Chem. Soc.* **2009**, *132*, 725; e) M. Yin, J. Shen, G. O. Pflugfelder, K. Müllen, *J. Am. Chem. Soc.* **2008**, *130*, 7806; f) Z. Li, S. Wan, W. Y. Shi, M. Wei, M. Yin, W. Yang, D. G. Evans, X. Duan, *J. Phys. Chem. C.* **2015**, *119*, 7428.
[8] L. Wu, Y. Dai, G. Marriott, *Org. Lett.* **2011**, *13*, 2018.
[9] Y. Wang, X. Tan, Y.-M. Zhang, S. Zhu, I. Zhang, B. Yu, K. Wang, B. Yang, M. Li, B. Zou, *J. Am. Chem. Soc.* **2015**, *137*, 931.
[10] D. Tong, H. Duan, J. Wang, Z. Yang, Y. Lin, *Sensor Actuator B-Chem.* **2014**, *195*, 80.
[11] G. Crini, *Chem. Rev.* **2014**, *114*, 10940.
[12] L. Yang, H. Zhang, T. Tan, A. U. Rahman, *J. Chem. Technol. Biotechnol.* **2009**, *84*, 611.
[13] G.-F. Yang, H.-B. Wang, W.-C. Yang, D. Gao, C.-G. Zhan, *J. Phys. Chem. B.* **2006**, *110*, 7044.
[14] Y.-J. Hu, Y. Liu, X.-H. Xiao, *Biomacromolecules* **2009**, *10*, 517.
[15] T. E. Kaiser, H. Wang, V. Stepanenko, F. Würthner, *Angew. Chem. Int. Ed.* **2007**, *46*, 5541.
[16] A. R. Khan, P. Forgo, K. J. Stine, V. T. D'Souza, *Chem. Rev.* **1998**, *98*, 1977.
[17] M. K. Beyer, H. Clausen-Schaumann, *Chem. Rev.* **2005**, *105*, 2921.